Solvation and Rotational Dynamics of Coumarin 153 in Ionic Liquids: Comparisons to Conventional Solvents

ARTICLE *in* THE JOURNAL OF PHYSICAL CHEMISTRY B · JUNE 2007

Impact Factor: 3.3 · DOI: 10.1021/jp070923h · Source: PubMed

Solvation and Rotational Dynamics of Coumarin 153 in Ionic Liquids: Comparisons to Conventional Solvents

Hui Jin,[†] Gary A. Baker,[‡] Sergei Arzhantsev,[†] Jing Dong,[†] and Mark Maroncelli*[,†]

Department of Chemistry, The Pennsylvania State University, 104 Chemistry Building, University Park, Pennsylvania 16802, and Chemical Sciences Division, Oak Ridge National Laboratory, P.O. Box 2008, Oak Ridge, Tennessee 37831-6110

Received: February 2, 2007; In Final Form: April 3, 2007

Steady-state and time-resolved emission spectroscopy with 25 ps resolution are used to measure equilibrium and dynamic aspects of the solvation of coumarin 153 (C153) in a diverse collection of 21 room-temperature ionic liquids. The ionic liquids studied here include several phosphonium and imidazolium liquids previously reported as well as 12 new ionic liquids that incorporate two homologous series of ammonium and pyrrolidinium cations. Steady-state absorption and emission spectra are used to extract solvation free energies and reorganization energies associated with the $S_0 \leftrightarrow S_1$ transition of C153. These quantities, especially the solvation free energy, vary relatively little in ionic liquids compared to conventional solvents. Some correlation is found between these quantities and the mean separation between ions (or molar volume). Time-resolved anisotropies are used to observe solute rotation. Rotation times measured in ionic liquids correlate with solvent viscosity in much the same way that they do in conventional polar solvents. No special frictional coupling between the C153 and the ionic liquid solvents is indicated by these times. But, in contrast to what is observed in most low-viscosity conventional solvents, rotational correlation functions in ionic liquids are nonexponential. Time-resolved Stokes shift measurements are used to characterize solvation dynamics. The solvation response functions in ionic liquids are also nonexponential and can be reasonably represented by stretched-exponential functions of time. The solvation times observed are correlated with the solvent viscosity, and the much slower solvation in ionic liquids compared to dipolar solvents can be attributed to their much larger viscosities. Solvation times of the majority of ionic liquids studied appear to follow a single correlation with solvent viscosity. Only liquids incorporating the largest phosphonium cation appear to follow a distinctly different correlation.

1. Introduction

Research exploring the uses of room-temperature ionic liquids is growing at an exponential pace. A recent news article lists solvents for nucleoside chemistry and biosensing, liquid rocket propellants, high-temperature lubricants, and index matching fluids as just some of the newest applications of ionic liquids.[1] In parallel with the these developing applications, much recent work has focused on characterizing the physical properties of ionic liquids and how they differ from those of conventional organic solvents.[2−5] One important aspect of the latter work involves attempts to understand the unique features of solvation in ionic liquids, using both thermodynamic[6−11] and spectroscopic methods.[8,11−13] In addition to equilibrium aspects of solvation, a number of groups have applied various techniques to measure dynamical aspects of solvation such as translational[14−16] and rotational[17−29] diffusion of solutes and measurements of solvation dynamics, the time-dependent response to a solute perturbation.[30,31] Study of the latter dynamics has been especially popular,[18−22,26−29,32−45] and several papers have just been published reviewing the status of this area.[38,46,47]

In the present paper we add to the growing literature on solvation in ionic liquids through spectroscopic measurements on the solvatochromic probe coumarin 153 (C153; Scheme 1) in a diverse collection of 21 ionic liquids. This work collects data previously reported by our group on a number of imidazolium[19,21] and phosphonium[20] ionic liquids together with new data on two homologous series of ammonium and pyrrolidinium ionic liquids. In addition to summarizing the ionic liquid results, a focus of the present work is to compare the solvation of C153 in ionic liquids and conventional dipolar solvents. We use steady-state absorption and emission data to measure solvent contributions to the free energy difference and reorganization energy associated with the $S_0 \leftrightarrow S_1$ transition of C153. In conventional dipolar solvents these equilibrium solvation quantities are well described by dielectric continuum models of solvation. On the basis of the data currently available on the dielectric constants of ionic liquids,[48−50] it appears that the same models are not useful for predicting the energetics in these solvents. Reasonable correlations are, however, observed for these energies with ion size. Time-resolved anisotropy measurements made with the time-correlated single photon counting (TCSPC) method are used to measure the reorientation of C153. In both conventional solvents and in ionic liquids the rotation times follow simple hydrodynamic predictions to a reasonable degree of accuracy. We find no evidence for the frictional coupling between this dipolar solute and its environment being qualitatively different in ionic liquids compared to conventional dipolar solvents. Finally, TCSPC measurements of the dynamic

* Author to whom correspondence should be addressed. E-mail: Maroncelli@psu.edu.
[†] The Pennsylvania State University.
[‡] Oak Ridge National Laboratory.

10.1021/jp070923h CCC: $37.00
Published on Web 05/27/2007

SCHEME 1

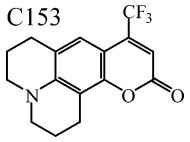

Stokes shift of C153 are used to quantify solvation dynamics in ionic liquids. It has been recognized for some time[18] that, despite the fact that slow dynamics are often observed, a substantial fraction of the solvation response is missed in such experiments, which are limited in our case by a 25 ps instrument response time. Fortunately, recent work with higher time resolution[38] indicates that the integral solvation times measured with TCSPC provide good estimates of the noninertial portions of the dynamics. Comparisons of these times measured in ionic liquids with the equivalent times in dipolar solvents reveals a single overall correlation between solvation time and solvent viscosity, albeit a very crude one. In ionic liquids, the connection between viscosity and solvation time appears to be much closer, especially if some account is made for ion size.

2. Materials and Experimental Methods

The 21 ionic liquids surveyed in this work are listed in Table 1. Structural formulas of the ions involved and the designations that we employ for them are described in Figure 1. 1-Butyl-3-methylimidazolium chloride [Im_{41}^+][Cl^-], 1-butyl-3-methylimidazolium hexafluorophosphate [Im_{41}^+][PF_6^-], 1-butyl-3-methylimidazolium bis(trifluoromethylsulfonyl)imide [Im_{41}^+][Tf_2N^-], 1-butyl-3-methylimidazolium tris(trifluoromethylsulfonyl)methide [Im_{41}^+][Tf_3C^-], and 1-propyl-2,3-dimethylimidazolium bis(trifluoromethylsulfonyl)imide [mIm_{31}^+][Tf_2N^-] were obtained from Covalent Associates (electrochemical grade, >99.5%, <50 ppm H_2O) and used as received. 1-Butyl-3-methylimidazolium tetrafluoroborate [Im_{41}^+][BF_4^-] was obtained from Sigma-Aldrich (97%). It was dissolved in acetonitrile and treated with activated carbon, after which the solvent was removed and the sample was dried under vacuum for 36 h at 60 °C. Methyl(tributyl)ammonium bis(trifluoromethylsulfonyl)imide [N_{4441}^+][Tf_2N^-] was provided by Pedatsur Neta and was synthesized according to the procedure described in ref 51. All liquids containing the trihexyl(tetracdecyl)-phosphonium ($P_{14,666}^+$) cation (~94%) were prepared by Cytec Canada.[52] The two series of liquids consisting of *N*-methyl(*N*-alkyl)pyrrolidinium (Pr_{n1}^+) and (dimethyl)(isopropyl)(alkylammonium) (N_{ipn11}^+) cations and the bis(trifluoromethylsulfonyl)-imide anion were synthesized according to published methods[53] and purified as detailed in ref 54. Coumarin 153 (laser grade) was purchase from Exciton and used as received.

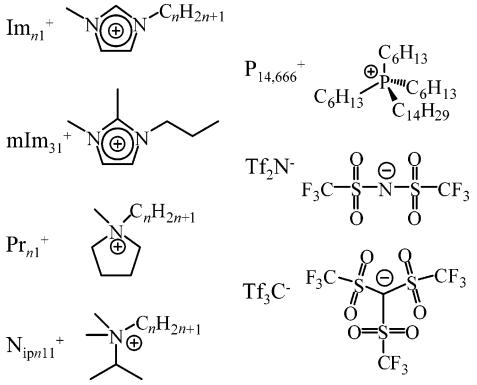

Figure 1. Structures of the ionic liquids surveyed and the designations employed in this work.

The physical properties and water contents of many of these ionic liquids will be detailed in a separate publication.[54] In most cases spectroscopic measurements were made on initially dried samples that were stored in a dry atmosphere but were not dried immediately prior to measurement. Such treatment means that the water content of most of the samples reported here varies between 100 and 500 ppm by weight. Exceptions are the phosphonium ionic liquids,[55] which contained up to 0.8% water (see ref 20), and the imidazolium chlorides, which contained 1−2% water. These higher amounts of water can significantly alter some physical properties such as viscosity. However, as discussed previously,[20] we have found that the spectra of C153 are not specifically sensitive to the presence of water, and the influence of water on the dynamics measured with C153 appear to be accounted for by viscosity changes alone. In all of the dynamical comparisons we therefore use viscosities measured using the same ionic liquids used for the time-resolved spectroscopic measurements.

The instrumentation and procedures for measuring steady-state and time-resolved spectral data are essentially the same as those described in ref 20. Absorption spectra (1 nm resolution)

TABLE 1: Ionic Liquids Studied (25 °C) and Some of their Characteristics

no.	ionic liquid	R_+ (Å)	R_- (Å)	M_w (g mol^{-1})	V_{vdW} (Å^3)	V_m (Å^3)	η (cP)	source, references
1	[Im_{41}^+][Cl^-]	3.39	2.09	175	202	269	~870	Covalent
2	[Im_{41}^+][BF_4^-]	3.39	2.29	226	214	313	75	Aldrich
3	[Im_{41}^+][PF_6^-]	3.39	2.72	284	248	345	187	ref 21 (Covalent)
4	[Im_{41}^+][Tf_2N^-]	3.39	3.39	419	326	491	41	Covalent
5	[Im_{41}^+][Tf_3C^-]	3.39	3.81	550	394	585	264	Covalent
6	[Im_{61}^+][Cl^-]	3.57	2.09	203	225	326	665	this work
7	[mIm_{31}^+][Tf_2N^-]	3.33	3.39	419	317	479	80	ref 19 (Covalent)
8	[Pr_{31}^+][Tf_2N^-]	3.41	3.39	408	329	483	53	ref 54
9	[Pr_{41}^+][Tf_2N^-]	3.47	3.39	422	337	526	70	ref 54
10	[Pr_{61}^+][Tf_2N^-]	3.71	3.39	450	377	568	93	ref 54
11	[$Pr_{10,1}^+$][Tf_2N^-]	4.10	3.39	507	451	674	145	ref 54
12	[N_{ip311}^+][Tf_2N^-]	3.41	3.39	410	328	488	105	ref 54
13	[N_{ip411}^+][Tf_2N^-]	3.58	3.39	410	355	517	130	ref 54
14	[N_{ip611}^+][Tf_2N^-]	3.76	3.39	438	386	563	139	ref 54
15	[$N_{ip10,11}^+$][Tf_2N^-]	4.16	3.39	509	464	718	154	ref 54
16	[N_{4441}^+][Tf_2N^-]	4.00	3.39	481	430	629	520	ref 19 (Neta)
17	[$P_{14,666}^+$][Cl^-]	5.34	2.09	519	676	978	1746	refs 20 and 52 (Cytec)
18	[$P_{14,666}^+$][Br^-]	5.34	2.26	564	686	983	1313	refs 20 and 52 (Cytec)
19	[$P_{14,666}^+$][BF_4^-]	5.34	2.29	571	688	993	780	refs 20 and 52 (Cytec)
20	[$P_{14,666}^+$][$N(CN)_2^-$]	5.34	2.51	550	704	1015	196	refs 20 and 52 (Cytec)
21	[$P_{14,666}^+$][Tf_2N^-]	5.34	3.39	764	800	1186	284	refs 20 and 52 (Cytec)

were recorded using a Hitachi U-3000 UV/vis spectrometer, and steady-state emission spectra were recorded with a Spex Fluorolog 212 spectrometer (2 nm resolution). Emission spectra were corrected for instrument responsivity calibrated against a series of dyes as described in ref 56. Time-resolved emission decays were measured using a TCSPC instrument[57] based on a femtosecond Ti:sapphire laser (Coherent Mira). The doubled output of this laser at 410 nm (~200 fs, 76 MHz) was used in the present measurements. Instrumental parameters were typically chosen to collect data at intervals of 4.8 ps over a total time of 20 ns, and data accumulated until a maximum of 1000−4000 counts were collected in the peak channel. To obtain time-resolved spectra, 14−16 decays at wavelengths spanning the emission spectrum (450−650 nm) were recorded at the magic angle through a monochromator with 8 nm resolution. The effects of instrumental broadening were partially removed from the data by independently fitting each decay to a sum of 3−4 exponentials using an iterative reconvolution scheme and an instrument response function (~25 ps full width at half-maximum (fwhm)) obtained from a scattering solution. Time-resolved spectra were then reconstructed from these fitted decays by normalizing to steady-state emission spectra in the usual manner.[58] Information about reorientational dynamics was obtained from a set of three decays measured near the peak of the steady-state emission and recorded with parallel, perpendicular, and magic angle polarizations. The parallel and perpendicular decays were simultaneously fit using an iterative reconvolution algorithm[59] to model functions including multi-exponential population decay and multiexponential or stretched-exponential anisotropy. All measurements were made in tightly sealed 1 cm quartz cuvettes using probe concentrations chosen to give optical densities near 0.1. Sample temperatures (±0.1 K) were controlled using circulating water from thermostated baths (Neslab).

3. Results and Discussion

A. Solvation Energies. Many workers have already attempted to characterize the polarity of ionic liquids using the spectral shifts of popular solvatochromic probes. In most cases electronic absorption has been used for this purpose[3,8] on such well-known probes as betaine 30,[13,60] the nitrobenzene derivatives used for the π^* scale,[61,62] Nile Red,[54,63,64] and others.[65,66] Coumarin 153 is in some ways a superior probe, because the possibility of measuring both absorption and emission shifts enables a finer definition of what is meant by solvent polarity. In particular, the Stokes shift of C153 has been shown to provide a direct measure of the "nuclear polarizability" of a solvent, i.e., that part of the solvent response due to positional and orientational reorganization of the permanent charge distributions of solvent molecules.[31,67]

Figure 2 provides a comparison of the absorption and emission spectra of C153 in a series of dipolar aprotic solvents of increasing polarity (2-methylbutane to dimethylsulfoxide) and in a representative ionic liquid, $[Pr_{31}^+][Tf_2N^-]$. As noted previously with respect to a number of other probes,[18,68] there is nothing distinctive about the spectra of C153 in ionic liquids. As illustrated by the $[Pr_{31}^+][Tf_2N^-]$ spectra here, the shift and broadening of the spectra of C153 in ionic liquids are indistinguishable from what pertains in strongly dipolar solvents. The example in Figure 2 is also typical in showing spectra that fall in the polarity range between acetone and dimethylsulfoxide.

Frequency data for all of the ionic liquids studied here are summarized in Table 2. This table contains peak frequencies of the absorption and steady-state emission spectra (ν_{abs}^{pk} and

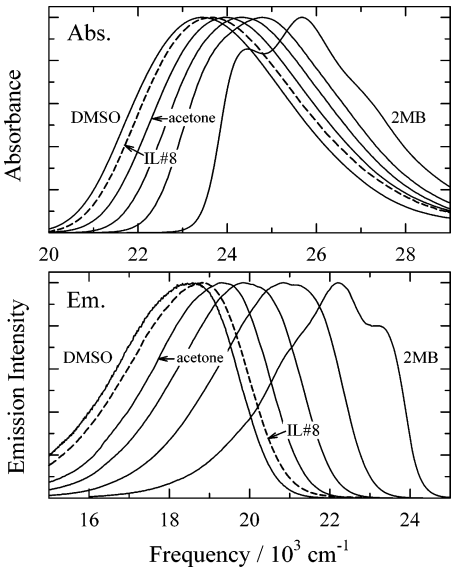

Figure 2. Absorption and emission spectra of C153 in representative conventional solvents (solid curves, data from ref 31) and in the ionic liquid $[Pr_{31}^+][Tf_2N^-]$ (dashed curves, 25 °C). All spectra are normalized to unit height. The conventional solvents are from right to left: 2-methylbutane (2MB), diethyl ether, ethyl acetate, acetone, and dimethylsulfoxide (DMSO).

ν_{em}^{pk}) as well as estimates of the peak frequency of the "time-zero", $\nu^{pk}(0)$, and fully relaxed spectra, $\nu^{pk}(\infty)$. Time-zero spectra were derived from an analysis of the shift and broadening of the absorption spectrum in a given ionic liquid relative to the spectrum in a nonpolar reference solvent, 2-methylbutane, as described in ref 69. Such spectra provide estimates of the emission prior to any solvent motion. Estimates of the spectra expected after full solvent relaxation were obtained by extrapolating the time-dependent data discussed in subsection 3C. We note that solvation in many of the ionic liquids is sufficiently slow compared to the ~6 ns emission lifetime of C153 that ν_{em}^{pk} is significantly larger than $\nu^{pk}(\infty)$; i.e., the steady-state emission spectrum does not provide a quantitative reflection of their equilibrium polarity. On average the difference is about 300 cm^{-1}.

From frequency data such as these we compute two solvation characteristics of the $S_0 \leftrightarrow S_1$ transition of C153, the solvation free energy difference

$$\Delta_{sol}G = \frac{1}{2}h\{\upsilon_{abs} + \upsilon(\infty)\} - \Delta G_0 \qquad (3.1)$$

and the reorganization energy

$$\lambda_{sol} = \frac{1}{2}h\{\upsilon(0) - \upsilon(\infty)\} \qquad (3.2)$$

By subtracting an approximate gas-phase value of $\Delta G_0 \cong 295.9$ kJ/mol in eq 3.1 estimated from a dielectric extrapolation in conventional solvents, $\Delta_{sol}G$ represents the difference in solvation free energies of the S_1 and S_0 states of C153. Similarly, λ_{sol} provides an approximate measure of the solvent contribution to the nuclear reorganization energy accompanying the $S_0 \leftrightarrow S_1$ transition. Values of $\Delta_{sol}G$ and λ_{sol} provided in Table 2 reflect weighted averages obtained by using both the peak frequencies listed there and also the first-moment frequencies (not tabulated) in eqs 3.1 and 3.2.

Figures 3 and 4 summarize these solvation energies and compare them to what is observed in conventional dipolar solvents. The energetics of C153 in dipolar solvents are well

TABLE 2: C153 Spectral Frequencies and Energy Estimates[a]

no.	ionic liquid	ν_{abs}^{pk} (10^3 cm^{-1})	ν_{em}^{pk} (10^3 cm^{-1})	$\nu_{est}^{pk}(0)$ (10^3 cm^{-1})	$\nu^{pk}(\infty)$ (10^3 cm^{-1})	$\Delta\nu_{est}^{pk}$ (10^3 cm^{-1})	λ_{sol} (kJ mol^{-1})	$-\Delta_{sol}G$ (kJ mol^{-1})
1	$[Im_{41}^+][Cl^-]$[b]	23.11	18.43	20.18	17.98	2.20	13.5	50.0
2	$[Im_{41}^+][BF_4^-]$	23.49	18.66	20.72	18.38	2.34	14.6	45.8
3	$[Im_{41}^+][PF_6^-]$	23.47	18.72	20.54	18.51	2.03	12.8	45.6
4	$[Im_{41}^+][Tf_2N^-]$	23.54	18.70	20.37	18.66	1.71	10.8	43.5
5	$[Im_{41}^+][Tf_3C^-]$	23.59	18.99	20.70	18.70	2.00	12.1	42.9
6	$[Im_{61}^+][Cl^-]$	23.32	18.89	20.54	18.38	2.16	13.3	46.5
7	$[mIm_{31}^+][Tf_2N^-]$	23.51	18.72	20.34	18.64	1.70	10.8	43.5
8	$[Pr_{31}^+][Tf_2N^-]$	23.66	18.84	20.79	18.66	2.13	13.0	43.0
9	$[Pr_{41}^+][Tf_2N^-]$	23.61	18.98	20.61	18.80	1.81	10.9	41.5
10	$[Pr_{61}^+][Tf_2N^-]$	23.53	18.96	20.59	18.75	1.84	11.1	43.4
11	$[Pr_{10,1}^+][Tf_2N^-]$	23.66	19.07	20.80	18.92	1.87	11.1	40.8
12	$[N_{ip311}^+][Tf_2N^-]$	23.54	18.77	20.73	18.63	2.10	13.2	43.5
13	$[N_{ip411}^+][Tf_2N^-]$	23.40	18.76	20.71	18.63	2.08	12.8	44.2
14	$[N_{ip611}^+][Tf_2N^-]$	23.64	19.01	20.82	18.79	2.03	12.6	42.0
15	$[N_{ip10,11}^+][Tf_2N^-]$	23.80	19.31	20.79	18.81	1.98	11.6	40.8
16	$[N_{4441}^+][Tf_2N^-]$	23.45	19.14	20.56	18.79	1.77	9.6	43.2
17	$[P_{14,666}^+][Cl^-]$[b]	23.19	19.59	20.27	18.70	1.58	9.6	47.0
18	$[P_{14,666}^+][Br^-]$[b]	23.34	19.19	20.25	18.68	1.58	9.6	47.4
19	$[P_{14,666}^+][BF_4^-]$[b]	23.27	19.36	20.31	18.90	1.41	8.6	45.3
20	$[P_{14,666}^+][N(CN)_2^-]$[b]	23.28	19.35	20.39	18.90	1.49	9.1	44.8
21	$[P_{14,666}^+][Tf_2N^-]$[b]	23.46	19.53	20.50	19.06	1.44	8.8	43.3

[a] ν_{abs}^{pk} and ν_{em}^{pk} are peak frequencies ($\pm$100 cm^{-1}) of the steady-state S_1 absorption and emission bands. $\nu_{est}^{pk}(0)$ is the estimated peak frequency of the "time-zero" spectrum, the spectrum expected prior to solvent relaxation, calculated via comparison of the absorption spectrum to the spectrum in a nonpolar reference solvent.[69] $\nu^{pk}(\infty)$ is the peak frequency of the fully relaxed spectrum, obtained by extrapolating time-resolved data to infinite time, and $\Delta\nu_{est} = \nu_{est}(0) - \nu(\infty)$. Uncertainties in the latter frequencies are estimated to be $\pm$200 cm^{-1}. λ_{sol} and $\Delta_{sol}G$ ($\pm$1$-$2 kJ/mol) are the solvent contributions to the reorganization energy and free energy change associated with the $S_0 \rightarrow S_1$ transition, calculated from frequency data as described in the text. [b] Most data were recorded at 298 K. Data in $[Im_{41}^+][Cl^-]$ are at 333 K, and the $[P_{14,666}^+]$ ionic liquids are at 343 K.

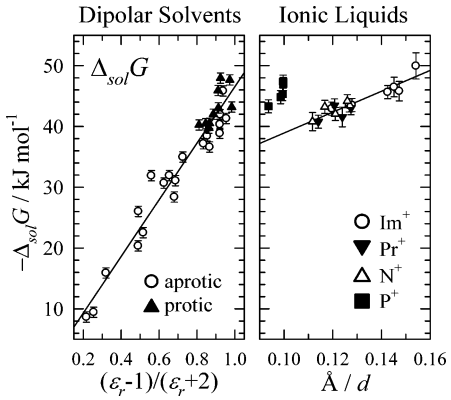

Figure 3. Solvation free energy differences ($S_1 - S_0$) of C153 in conventional dipolar liquids and in ionic liquids. The left panel shows data in 30 conventional dipolar solvents calculated using data from refs 31 and 67. The regression shown here is $\Delta_{sol}G$/kJ mol^{-1} = $-46.5f(\epsilon_r)$ ($r^2 = 0.995$, standard error = 2.6). The right panel shows ionic liquid data plotted vs the inverse of the mean ionic separation, $1/d = V_m^{-1/3}$. The line here is a fit to the ionic liquid data excluding the phosphonium liquids ($N = 16$, $r^2 = 0.84$).

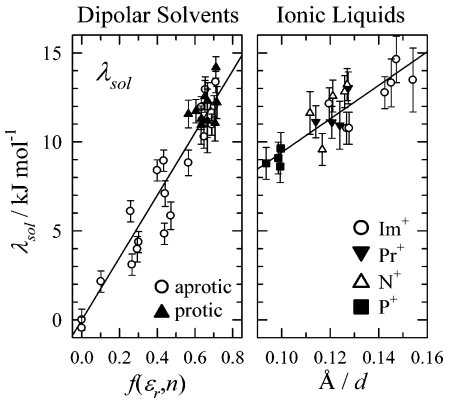

Figure 4. Solvent reorganization energies of C153 in conventional dipolar liquids and in ionic liquids. The left panel shows data in 30 conventional dipolar solvents calculated using data from refs 31 and 67. These data are plotted vs the function $f(\epsilon_r,n)$ defined by eq 3.3. The regression shown here is λ_{sol}/kJ mol^{-1} = $17.5f(\epsilon_r,n)$ ($r^2 = 0.98$, standard error = 1.2). The right panel shows ionic liquid data plotted vs the inverse of the mean ionic separation, $1/d = V_m^{-1/3}$. The regression here is λ_{sol}/kJ mol^{-1} = 94.2(Å/d) ($N = 21$, $r^2 = 0.74$, standard error = 0.9).

accounted for using simple continuum dielectric models of solvation.[31,67] This fact is illustrated by Figure 3, which shows that $\Delta_{sol}G$ in dipolar solvents is approximately proportional to the reaction field factor $(\epsilon_r - 1)/(\epsilon_r + 2)$, where ϵ_r is the relative permittivity of the solvent. To a good first approximation, the single parameter, ϵ_r, captures the net (nuclear + electronic) polarizabilities of conventional dipolar solvents relevant for determining $\Delta_{sol}G$. It is noteworthy that there is no distinction between the behavior of protic and aprotic solvents in Figure 3 (or Figure 4), which indicates that the $S_0 \leftrightarrow S_1$ transition of C153 primarily senses the strength of nonspecific polar interactions and is insensitive to hydrogen bonding.

The values of $\Delta_{sol}G$ in the ionic liquids studied here all fall within a relatively narrow range between 40 and 50 kJ/mol. This modest spread, a factor of 5 smaller than that observed in dipolar solvents, is surprising given the variety of ionic liquids included in this study. To date, the relative permittivities of only five of these ionic liquids (2, 3, 4, 7, and 9) have been determined,[48,70] and they too fall within a remarkably narrow range, $11.1 \leq \epsilon_r \leq 11.9$.[71] However, these values of ϵ_r are all smaller than would be expected if the same correlation found in dipolar liquids was to apply to ionic liquids. This correlation would imply values in the range $19 \leq \epsilon_r \leq \infty$. Given the different character of the electrostatics, it is not surprising that the same correlation does not apply to both classes of liquids. In fact, one might anticipate that ϵ_r, which monitors dipolar interactions, would fail to account for the most important aspects of the electrostatic interactions present in ionic liquids, in much the same way that it fails in quadrupolar solvents.[67,72]

In the absence of any theory of dipolar solvation in ionic liquids, we have plotted the observed values of $\Delta_{sol}G$ in ionic liquids versus the inverse of the average ion−ion separation, calculated from the experimental molar volumes using $1/d = V_m^{-1/3}$. We adopt this particular parameter as a measure of the strength of electrical interactions by analogy to its appearance in the Born−Lande expression for lattice energies of ionic crystals. More generally, V_m has been found to correlate both energetic and entropic properties of ionic substances.[73] As indicated by the solid line in Figure 3, some correlation seems to exist between $1/d$ and $\Delta_{sol}G$ in the majority of the ionic liquids studied here, but this correlation does not extend to the liquids containing the large $P_{14,666}^+$ cation. One might imagine electronic polarizability also to be important in determining $\Delta_{sol}G$. But attempts to include electronic polarizability using the refractive indices of the ionic liquids[54] did not provide better correlations.

Figure 4 shows an analogous presentation of solvent reorganization energies, λ_{sol}. In dipolar solvents, the reorganization energies of C153 are approximately proportional to dielectric measures of nuclear solvent polarizability such as

$$f(\epsilon_r,n) = \frac{\epsilon_r - 1}{\epsilon_r + 2} - \frac{n^2 - 1}{n^2 + 2} \qquad (3.3)$$

As was the case with $\Delta_{sol}G$, hydrogen bonding in conventional solvents does not appear to affect these energies. The values of λ_{sol} observed in ionic liquids cover a greater fraction of the range spanned by dipolar solvents than did the $\Delta_{sol}G$ values. If the same correlation with ϵ_r found in dipolar solvents were to pertain to the ionic liquids, then the range of dielectric constants implied would be $10 \leq \epsilon_r \leq \infty$. For the collection of ionic liquids mentioned above whose relative permittivities have been measured to be 11.5 ± 0.4, the observed values of λ_{sol} imply that $\epsilon_r \geq 65$. Thus, here too, if any simple relationship between λ_{sol} and ϵ_r exists, it must differ from that applicable to conventional solvents. However, as illustrated in Figure 4, the parameter $1/d$ does correlate the reorganization energies of ionic liquids to within their expected uncertainties. Thus, it appears that it should be possible to model solvent reorganization energies in ionic liquids in a manner comparable to dielectric continuum models in conventional solvents by using some parameter, such as $1/d$, related to ion densities or molar volumes.

B. Rotational Dynamics. Figure 5 displays a representative set of anisotropy data recorded for C153 in $[Pr_{31}^+][Tf_2N^-]$. As is the case here, we mainly collect anisotropy information near the peak of the steady-state emission spectrum, where magic angle or population decays "$K(t)$" are usually close to single-exponential functions of time. The simplicity of the decays in this spectral region facilitates accurate anisotropy fits. We also have examined anisotropies at wavelengths on the blue and red edges of the steady-state emission spectrum in a number of liquids and find the same anisotropy decays $r(t)$ to within anticipated uncertainties. In addition, in the particular liquid, $[N_{ip311}^+][Tf_2N^-]$, we measured anisotropy data at a number of excitation wavelengths and observed no dependence upon excitation wavelength.[74] Thus, at least for many of the ionic liquids studied here, we do not find any clear evidence for heterogeneity in the rotational dynamics of C153.

We fit anisotropy decay data to both stretched-exponential

$$r(t) = r_0 \exp\{-(t/\tau_{0r})^{\beta_{rot}}\} \qquad (3.3)$$

and biexponential functions of time, using a fixed value of the initial anisotropy, $r_0 = 0.375$.[75] As in the example shown in Figure 5, the stretched-exponential representation typically afforded good fits to such data. In only a few cases did the additional fitting parameter available with a biexponential function provide better fits, at least at the signal-to-noise levels used in the present study. However, we note that recent work by Castner and co-workers[29] on C153 in comparable ionic liquids has shown that when data are collected over a wider time window (>50 ns) and with higher signal-to-noise, three- or even four-exponential representations may be needed to fit anisotropy data. For this reason we do not ascribe any meaning to the stretched-exponential function or its parameters here. Instead we use it as a convenient way to approximately represent the data.

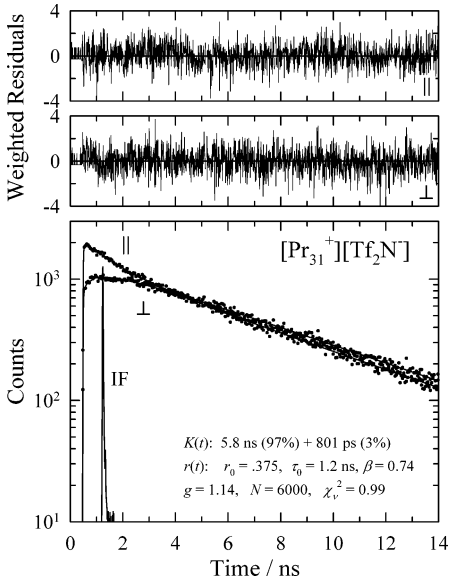

Figure 5. Representative anisotropy decay data in $[Pr_{31}^+][Tf_2N^-]$ at 313 K ($\lambda_{em} = 530$ nm, $\lambda_{exc} = 410$ nm). The bottom panel shows data (points) recorded with the analyzing polarizer parallel (||) and perpendicular (⊥) to the excitation polarization direction as well as fits to these data (solid curves). The curve labeled "IF" is the instrument response function. The top panels show the weighted residuals and the parameters of the biexponential fit to the population decay function $K(t)$ and a stretched-exponential fit to the anisotropy decay function $r(t)$. g is the parallel to perpendicular sensitivity factor, N is the total number of points in the fit, and χ_ν^2 is the goodness of fit parameter. Residuals have been thinned by a factor of 2, and data points by a factor of 10 for clarity.

Table 3 contains a summary of the parameters τ_{0r} and β_{rot} from stretched-exponential fits as well as rotational correlation times $\langle\tau_{rot}\rangle$ (the integral of $r(t)/r_0$) determined by averaging values obtained from both stretched-exponential and biexponential fits. The uncertainties listed in $\langle\tau_{rot}\rangle$ partially reflect the differences in the times obtained by these two fitting methods. In general, the values of β_{rot} observed here indicate a significantly nonexponential character to the reorientational correlation functions. This nonexponentiality is somewhat unusual in the sense that hydrodynamic modeling[76] predicts exponential anisotropies. At least in low-viscosity solvents, C153 does rotate exponentially. However, studies in conventional solvents have shown that reorientational correlation functions of C153 are often nonexponential in slowly relaxing solvents such as the normal alcohols.[76,77] We conjectured previously that such nonexponential dynamics reflect the non-Markovian character of rotational friction in slowly relaxing solvents.[76] Such an explanation is also plausible in ionic liquids, but dynamic heterogeneity might also be the source of this behavior, at least in some instances.

TABLE 3: Summary of Dynamical Quantities[a]

				rotation					solvation			
no.	ionic liquid	T (K)	η (cP)	τ_{0r} (ns)	β_{rot}	$\langle\tau_{rot}\rangle$ (ns)	C_{rot}	$\Delta\nu$ (10^3 cm^{-1})	f_{obs}	τ_{0s} (ns)	β_{solv}	$\langle\tau_{solv}\rangle$ (ns)
1	$[Im_{41}^+][Cl^-]$	333	300	10.2	0.69	13 ± 3	0.46	1.00	0.45	0.61	0.54	1.1 ± 0.3
2	$[Im_{41}^+][BF_4^-]$	298	75	4.1	0.76	4.3 ± 0.6	0.56	0.99	0.40	0.34	0.72	0.42 ± 0.06
3	$[Im_{41}^+][PF_6^-]$[b]	283	492					1.42	0.73	1.2	0.44	3.0 ± 0.6
3	$[Im_{41}^+][PF_6^-]$[b]	293	251					1.50	0.75	0.64	0.44	1.7 ± 0.3
3	$[Im_{41}^+][PF_6^-]$[b]	298	187	9.3	0.69	12.0 ± 2.4	0.63	1.37	0.68	0.50	0.49	1.03 ± 0.10
3	$[Im_{41}^+][PF_6^-]$	298	187	10.7	0.73	12.0 ± 2.4	0.62	1.26	0.62	0.71	0.69	1.00 ± 0.15
3	$[Im_{41}^+][PF_6^-]$	318	71	4.6	0.75	5.8 ± 0.9	0.85	1.05	0.49	0.30	0.73	0.36 ± 0.05
3	$[Im_{41}^+][PF_6^-]$[b]	343	29	0.81	0.75	0.99 ± 0.15	0.38	0.93	0.45	0.11	0.73	0.14 ± 0.02
4	$[Im_{41}^+][Tf_2N^-]$[c]	298	42	2.1	0.77	2.6 ± 0.4	0.61	0.94	0.54	0.23	0.74	0.28 ± 0.04
5	$[Im_{41}^+][Tf_3C^-]$	293	370					1.51	0.73	1.08	0.55	1.9 ± 0.6
5	$[Im_{41}^+][Tf_3C^-]$	298	267	15.2	0.65	20 ± 5	0.73					
5	$[Im_{41}^+][Tf_3C^-]$	313	112	5.3	0.65	5.3 ± 1.6	0.49	1.43	0.71	0.36	0.66	0.50 ± 0.10
5	$[Im_{41}^+][Tf_3C^-]$	333	47	1.5	0.67	1.8 ± 0.3	0.42	1.30	0.65	0.17	0.67	0.22 ± 0.03
6	$[Im_{61}^+][Cl^-]$	298	664	43	0.46	70 ± 30	1.0	1.55	0.70	2.49	0.54	4.4 ± 0.7
7	$[mIm_{31}^+][Tf_2N^-]$[c]	263	760					1.62	0.84	2.10	0.37	9.1 ± 2.0
7	$[mIm_{31}^+][Tf_2N^-]$[c]	273	340					1.43	0.76	0.98	0.44	2.6 ± 0.6
7	$[mIm_{31}^+][Tf_2N^-]$[c]	283	180	11.0	0.66	15 ± 3	0.77	1.02	0.57	0.69	0.57	1.10 ± 0.20
7	$[mIm_{31}^+][Tf_2N^-]$[c]	298	80	3.6	0.74	4.3 ± 0.6	0.52	0.99	0.56	0.32	0.63	0.45 ± 0.05
7	$[mIm_{31}^+][Tf_2N^-]$[c]	323	31	1.10	0.77	1.30 ± 0.20	0.44	0.80	0.46	0.14	0.80	0.16 ± 0.03
8	$[Pr_{31}^+][Tf_2N^-]$	298	53	2.4	0.75	2.6 ± 0.4	0.47	1.28	0.57	0.20	0.65	0.28 ± 0.04
8	$[Pr_{31}^+][Tf_2N^-]$	313	43	1.25	0.74	1.41 ± 0.21	0.33	1.19	0.56	0.17	0.64	0.23 ± 0.05
8	$[Pr_{31}^+][Tf_2N^-]$	333	17	0.58	0.77	0.65 ± 0.10	0.41	1.14	0.52	0.07	0.66	0.094 ± 0.014
9	$[Pr_{41}^+][Tf_2N^-]$	298	70	3.1	0.71	3.4 ± 0.5	0.47	1.24	0.68	0.26	0.61	0.38 ± 0.06
10	$[Pr_{61}^+][Tf_2N^-]$	298	93	4.0	0.68	5.7 ± 0.9	0.61	1.44	0.78	0.35	0.56	0.59 ± 0.09
11	$[Pr_{10,1}^+][Tf_2N^-]$	298	145	5.8	0.61	9.0 ± 1.3	0.60	1.44	0.77	0.73	0.54	1.3 ± 0.3
12	$[N_{ip311}^+][Tf_2N^-]$	298	105	4.6	0.72	4.4 ± 1.1	0.41	1.26	0.57	0.35	0.62	0.51 ± 0.07
13	$[N_{ip411}^+][Tf_2N^-]$	298	130	6.0	0.67	7.9 ± 1.2	0.60	1.39	0.65	0.38	0.56	0.64 ± 0.09
14	$[N_{ip611}^+][Tf_2N^-]$	298	139	5.4	0.63	7.8 ± 1.2	0.55	1.43	0.68	0.64	0.61	0.97 ± 0.15
15	$[N_{ip10,11}^+][Tf_2N^-]$	298	155	7.1	0.73	9.2 ± 1.4	0.58	1.81	0.92	1.4	0.62	2.0 ± 1.0
15	$[N_{ip10,11}^+][Tf_2N^-]$	313	73	4.0	0.79	5.0 ± 0.7	0.70	1.58	0.83	1.2	0.66	1.6 ± 0.5
16	$[N_{4441}^+][Tf_2N^-]$[c]	298	520	17	0.41	51 ± 25	1.0	1.55	0.97	1.30	0.39	4.5 ± 1.5
17	$[P_{14,666}^+][Cl^-]$[d]	331	230	1.3	0.36	6.0 ± 0.9	0.28	1.76	0.97	2.4	0.43	6.7 ± 1.7
17	$[P_{14,666}^+][Cl^-]$[d]	343	133	1.3	0.43	3.9 ± 0.6	0.33	1.50	0.93	1.9	0.46	4.5 ± 0.3
18	$[P_{14,666}^+][Br^-]$[d]	343	116	1.10	0.40	3.5 ± 0.5	0.34	1.59	0.99	1.3	0.38	5.1 ± 0.4
19	$[P_{14,666}^+][BF_4^-]$[d]	318	251	4.2	0.42	12 ± 2	0.50	1.57	1.03	3.5	0.41	11.3 ± 0.8
19	$[P_{14,666}^+][BF_4^-]$[d]	343	87	1.5	0.48	3.1 ± 0.5	0.40	1.37	0.95	1.01	0.51	1.98 ± 0.11
20	$[P_{14,666}^+][N(CN)_2^-]$[d]	343	31	0.91	0.54	1.60 ± 0.24	0.58	1.42	0.93	0.36	0.48	0.78 ± 0.05
21	$[P_{14,666}^+][Tf_2N^-]$[d]	298	277	7.5	0.46	18 ± 4	0.63	1.60	1.06	3.7	0.42	10.6 ± 0.6
21	$[P_{14,666}^+][Tf_2N^-]$[d]	318	102	2.8	0.50	5.5 ± 0.8	0.56	1.54	1.03	1.3	0.44	3.52 ± 0.23
21	$[P_{14,666}^+][Tf_2N^-]$[d]	343	39	1.00	0.56	1.7 ± 0.3	0.49	1.43	0.97	0.44	0.47	0.99 ± 0.06

[a] Viscosities η were calculated from parametrizations of temperature-dependent data reported in ref 54 or in the earlier references cited. τ_{0r} and β_{rot} are from stretched-exponential fits of anisotropy data (eq 3.3); $\langle\tau_{rot}\rangle$ is the rotational correlation time determined as an average of the results from both stretched-exponential and biexponential fits. C_{rot} is the rotational coupling factor defined by eq 3.5. $\Delta\nu$, τ_{0s}, and β_{solv} are the parameters of eq 3.6 averaged over $\nu(t)$ measured using both the peak and the first-moment measures of frequency. The integral solvation time $\langle\tau_{solv}\rangle$ is related to these values by $\langle\tau\rangle = \tau_0\Gamma(\beta^{-1})/\beta$ where Γ is the gamma function. f_{obs} (± 0.1) is the fraction of the expected solvation shift actually observed, $f_{obs} = \{\nu(0) - \nu(\infty)\}/\{\nu_{est}(0) - \nu(\infty)\}$. [b] Data from ref 21. [c] Data from ref 19. [d] Data from ref 20.

TABLE 4: Dynamic Characteristics Averaged over Cation Classes[a]

	no.	β_{rot}	C_{obs}	β_{solv}	f_{obs}
Im^+	12/18	0.71 ± 0.05	0.58 ± 0.15	0.60 ± 0.13	0.62 ± 0.13
Pr^+	6/6	0.71 ± 0.06	0.48 ± 0.11	0.61 ± 0.05	0.65 ± 0.11
N^+	5/6	0.71 ± 0.06	0.57 ± 0.10	0.58 ± 0.10	0.77 ± 0.16
P^+	9/9	0.46 ± 0.07	0.46 ± 0.12	0.44 ± 0.04	0.98 ± 0.05

[a] No. is the number of data sets (rotation/solvation) used in the averages. Values are the average over the cation class $\pm$ the standard deviation of each set. In computing the rotational averages data from liquids 6 and 16 have been omitted because of their much larger uncertainties.

There is a significant difference in the degree of nonexponentiality of the rotational anisotropy decays observed in the phosphonium ionic liquids compared to all of the other liquids studied. The distinction is most obvious in the cation-averaged data shown in Table 4. Here we list β_{rot} values averaged over data for the four different types of cations examined. It is clear from this summary that liquids incorporating the large phosphonium cation $P_{14,666}^+$ stand out as being markedly more nonexponential than the remaining types of liquids (see also Figure 4 of ref 20). The values of $\beta_{rot} \approx 0.7$ in the other ionic liquids indicate a degree of nonexponentiality that is roughly comparable to what was found for C153 in normal alcohol solvents.[76,77] The fact that we have failed to observe an excitation wavelength dependence for the rotation times of C153 in $[N_{ip311}^+][Tf_2N^-]$ (298 K, $\beta_{rot} = 0.72 \pm 0.01$ for $\lambda_{exc} = 410-460$ nm) suggests that in the majority of the ionic liquids studied here heterogeneity is not the main source of the nonexponential rotations. In the phosphonium liquids, however, rotational motion is highly dispersive ($\beta_{rot} \approx 0.5$) and similar to what is observed near the glass transition of fragile glass-forming liquids when the solute/solvent size ratio is small.[27,78,79] We conjecture that in these latter ionic liquids the large size of the cation relative to the solute ($V_{P^+}/V_{C153} \approx 2.6$) might produce dynamic heterogeneity similar to that observed in conventional glass-forming liquids. Alternatively, the heterogeneity might result from the domain-like structures observed in simulations of ionic

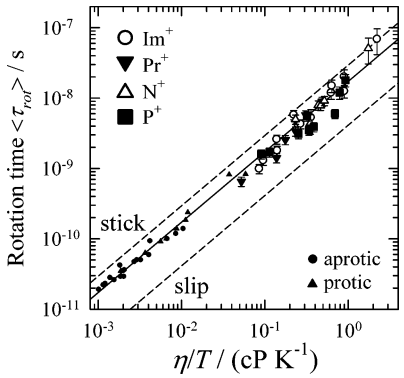

Figure 6. Rotational correlation times of C153 in 27 dipolar solvents at room temperature (small symbols, data from ref 76) and in ionic liquids (larger symbols with error bars) plotted vs η/T. The solid line shows the best fit of the dipolar liquid data to the proportionality $\langle\tau_{rot}\rangle = A(\eta/T)$ with $A = 1.73 \times 10^{-8}$ s K cP^{-1}. The dashed lines show the predictions of hydrodynamic calculations using slip and stick boundary conditions.

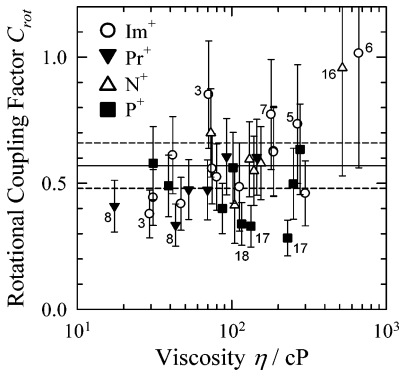

Figure 7. Rotational coupling factors of C153 measured in ionic liquids. The solid and dashed horizontal lines in this figure indicate the average and standard deviation of C_{rot} observed in the sample of dipolar liquids. The error bars here include the estimated uncertainties in both the rotation time and the viscosity (assumed to be ±10%). Numbers indicate ionic liquids according to Table 1.

liquids with long alkyl chains.[80,81] Whatever the origin, the character of the rotational correlation functions in the phosphonium liquids is decidedly different from those in the other liquids studied.

We now turn to the rotational correlation times of C153, $\langle\tau_{rot}\rangle = r_0^{-1} \int r(t)\, dt$. Figure 6 displays the results measured in ionic liquids and conventional solvents. Rotation times are plotted versus η/T (viscosity/temperature), the scaling expected from hydrodynamic models. The smaller points in Figure 6 are data in 27 dipolar solvents at room temperature, as taken from ref 76. The solid line in this figure shows that in dipolar solvents, both protic and aprotic and including the *n*-alcohols, rotation times of C153 conform to the expected proportionality to η/T, albeit with some scatter. The rotation times in ionic liquids show greater scatter but nevertheless also follow essentially the same correlation established by the dipolar solvents. The dashed lines in Figure 6 are the predictions of hydrodynamic models, made by assuming a solute of ellipsoidal shape with semi-axis dimensions of 2.0, 4.8, and 6.1 Å[76] and the relation

$$\tau^{(2)} = \frac{V\eta}{k_B T} fC \tag{3.4}$$

where V is the solute volume (246 Å^3), f is a shape factor (1.71), and C is a "rotational coupling factor". For stick boundary conditions $C = 1$, and for slip boundary conditions $C = 0.24$.[76] Virtually all of the rotation times, in both dipolar and ionic liquids, fall between these two limiting predictions.

A convenient way to examine deviations from hydrodynamic predictions is to calculate an empirical value of the coupling factor

$$C_{rot} = \frac{k_B T}{V\eta f} = \frac{\langle\tau_{rot}\rangle}{\tau^{(2)}_{stk}} \tag{3.5}$$

where $\tau^{(2)}_{stk}$ is the stick hydrodynamic prediction. In dipolar solvents we find $C_{rot} = 0.57 \pm 0.09$. Values of this factor in the ionic liquids are listed in Tables 3 and 4 and plotted in Figure 7. Neglecting liquids 6 and 16 whose long rotation times make the data highly uncertain, the average value of C_{rot} is 0.53 ± 0.13, close to the dipolar liquid value. Although there are several cases, for example, [$P_{14,111}^+$][Cl^-] and [$P_{14,111}^+$][Br^-] (17 and 18), where the deviations of C_{rot} from the dipolar liquid values are greater than the estimated uncertainties, most values of C_{rot} measured in the ionic liquids fall within the scatter of the dipolar liquid data (denoted by the dashed lines in Figure 7). Overall, these results indicate that there is no obvious difference between the way in which rotation of C153 is coupled to bulk viscosity in ionic liquids and in conventional dipolar solvents. Also, unlike β_{rot}, there is no clear distinction among the values of C_{rot} in the different cation classes (Table 4).

Finally it is worth mentioning how the present data compare to other data on rotation in the literature. Although there are few direct comparisons possible,[82] we can compare the general trends observed here to the recent data of Castner and co-workers[29] who measured rotation times of C153 in two ammonium and two pyrrolidimium ionic liquids at five temperatures between 278 and 353 K. In the two pyrrolidimium liquids these authors observed small-amplitude components with time constants of greater than 100 ns, which we would not be able to detect in the present experiments. If these slow components of uncertain origin are neglected, then the correlation times measured by Castner and co-workers[29] fall nicely on the correlation with η/T established here. For their set of 20 data points we find $C_{rot} = 0.46 \pm 0.06$, just slightly lower than our average ionic liquid value.

C. Solvation Dynamics. Representative time-resolved spectra of C153 in [N_{ip311}^+][Tf_2N^-] are shown in Figure 8. Unnormalized spectra in a wavelength representation are plotted in the upper panel. The spectra decrease in overall intensity due to the ~6 ns lifetime of C153 and simultaneously shift to the red in a manner characteristic of solvation dynamics. In the bottom panel these spectra have been normalized and fit to a log-normal line shape function[58] to illustrate the fact that there is little change in spectral width or shape with time. The dashed curve labeled "est. $t = 0$" is the estimated time-zero spectrum[69] discussed in subsection 3A, and "obs. $t = 0$" is what is observed from deconvolution analysis of the time-resolved data. The displacement between these two curves indicates that some portion (~40%) of the solvation response is missed in these experiments due to the finite response time of the TCSPC experiment (25 ps fwhm). As will be discussed more later, recent experiments having greater time resolution[37,38] have shown that this missing portion of the dynamics contains both subpicosecond inertial contributions as well as components relaxing on the 1−10 ps time scale. For now we note that in many of the ionic liquids studied here we can only partially characterize the solvation response with the present approach.

Quantitative information about the solvation response is derived from the time dependence of characteristic frequencies

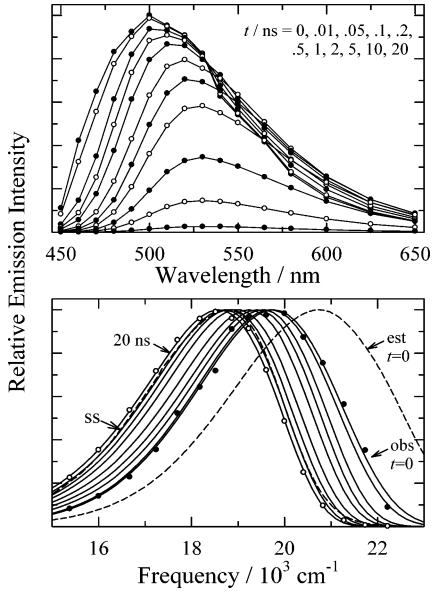

Figure 8. Time-resolved spectra of C153 in $[N_{ip311}^+][Tf_2N^-]$ at 298 K. The top panel contains reconstructed spectra at the times indicated. The bottom panel shows fits of these spectra in a frequency representation to log-normal line shape functions (smooth solid curves). The actual data at $t = 0$ and 20 ns are shown as filled and open symbols, respectively. The dashed curves labeled "ss" and "est. $t = 0$" are the steady-state and estimated "time-zero" spectra. In the bottom panel, spectra at 5 and 10 ns have been omitted for clarity.

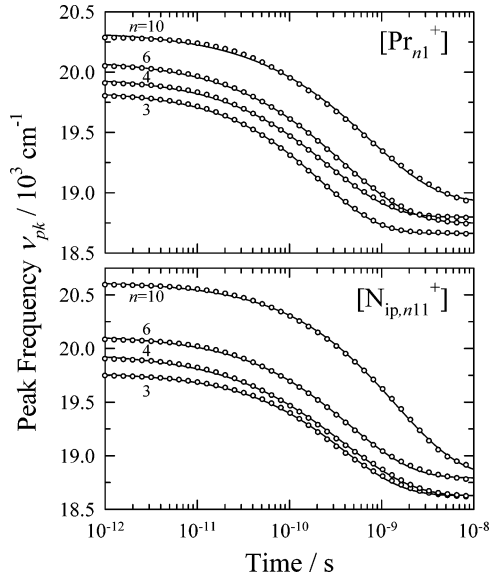

Figure 9. Representative peak frequency data $\nu_{pk}(t)$ obtained from log-normal fits of time-resolved spectra in the $[Pr_{n1}^+][Tf_2N^-]$ and $[N_{ipn11}^+][Tf_2N^-]$ series at 298 K. Points are the actual data, and the smooth curves are stretched-exponential fits (eq 3.6) to these data.

of the time-evolving spectra. Figure 9 shows the time evolution of the peak frequency $\nu_{pk}(t)$ of the fitted spectra of C153 in the two homologous series $[Pr_{n1}^+][Tf_2N^-]$ and $[N_{ipn11}^+][Tf_2N^-]$ with $n = 3$, 4, 6, and 10. These plots serve to illustrate the quality of the data recorded here. Assuming that it is reasonable to expect all features of these data to vary systematically with n, the fact that there is some crossover of the curves at long times suggests a precision of roughly ± 100 cm^{-1} in $\nu_{pk}(t)$. Repeated runs on the same liquid suggest similar uncertainties. The curves in Figure 9 are fits of the logarithmically spaced data (symbols) to a stretched-exponential time dependence

$$\nu(t) = \nu(\infty) + \Delta\nu \exp\{-(t/\tau_{0s})^{\beta_{solv}}\} \qquad (3.6)$$

As illustrated here, this functional form is able to reproduce the data to well within its anticipated accuracy. Although deviations in some data sets are larger than those shown in Figure 9, we find that such fits adequately capture the dynamics of $\nu(t)$ in all of the ionic liquids studied. Multiexponential representations, preferred by most other authors,[29,41,46] do fit some data sets more accurately, but they do so only at the expense of introducing additional fitting parameters that we find unnecessary.

In Table 3 we summarize all of the solvation dynamics measurements by listing quantities derived mainly from stretched-exponential fits to $\nu(t)$ data. $\Delta\nu$, τ_{0s}, and β_{solv} are the values of the parameters in eq 3.6 averaged over fits to $\nu(t)$ data using both the peak and the first-moment frequencies of the spectra. The integral solvation time $\langle\tau_{solv}\rangle$ is related to these values by $\langle\tau\rangle = \tau_0\Gamma(\beta^{-1})/\beta$ where Γ is the gamma function. f_{obs} is the fraction of the expected solvation shift actually observed, $f_{obs} = \Delta\nu/\{\nu_{est}(0) - \nu(\infty)\}$. Cation-averaged values of β and f_{obs} are also provided in Table 4.

The magnitudes of the Stokes shifts $\Delta\nu$ observed range between approximately 1000 and 2000 cm^{-1}. The fraction of the total solvation response represented by these Stokes shifts varies from about 0.5 to 1 depending on the solvent. As highlighted in Table 4, virtually all of the dynamics are observed in the $P_{14,111}^+$ liquids whereas successively less and less of the response is observed in the ammonium, pyrrolidinium, and imidazolium ionic liquids. Crudely speaking, these trends in f_{obs} are inversely related to the speed of the observed solvation response in the manner expected. Comparing values of β_{solv} and β_{rot} shows that generally $\beta_{solv} < \beta_{rot}$—the observed solvation response functions are usually farther from single-exponential functions than the rotational correlation functions in a given liquid. This observation is consistent with the behavior noted by Ito and Richert in two ionic liquids near their glass transitions.[26,27] Table 4 also suggests a significant difference in the degree of nonexponentiality (β_{solv}) among the different classes of ionic liquids, with the phosphonium liquids again being distinct in their larger departure from exponential time dependence. However, this last observation is probably an artifact related to the insufficient time resolution in the experiments. Values of β_{solv} are clearly correlated with f_{obs} (the set of all data shows a linear correlation coefficient of 0.75) such that the smaller the fraction of the response observed, the more exponential the response appears to be. (See, for example, the temperature-dependent series in the $[mIm_{31}^+][Tf_2N^-]$ liquid in Table 3.)

Data collected with sufficient time resolution to observe the entire solvation response[37,38] show that the nonexponentiality of even the noninertial component of the response is systematically underestimated by TCSPC experiments when f_{obs} is significantly less than unity. Thus, values of β_{solv} reported here are probably best viewed as upper limits to the correct values. Values of τ_{0s} measured by TCSPC were also found to be systematically too large when f_{obs} is much less than unity.[38] Luckily, the systematic biases created in β_{solv} and τ_{0s} as a result of insufficient time resolution work in opposite directions so as to partially cancel when the correlation time $\langle\tau_{solv}\rangle$ is considered. At least in the set of six ionic liquids fully resolved to date (2−6 and 8), the values of $\langle\tau_{solv}\rangle$ measured with TCSPC are found to deviate only by an average of 20% from values associated with the noninertial component of the dynamics.[38] We therefore focus solely on $\langle\tau_{solv}\rangle$ in the remaining discussion.

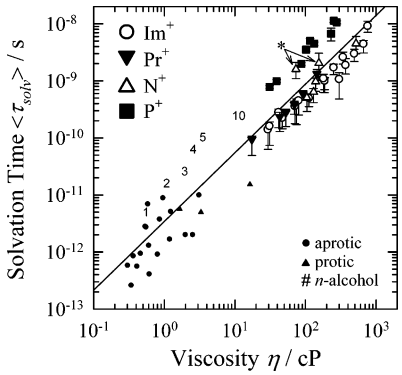

Figure 10. Integral solvation times $\langle\tau_{solv}\rangle$ in conventional dipolar solvents and in ionic liquids plotted vs solvent viscosity. The dipolar solvent data (small symbols and numerals) are from refs 31 and 67. Numerals n denote normal alcohols $C_nH_{2n+1}OH$. The ionic liquid data (large symbols with error bars) represent observed values of $\langle\tau_{solv}\rangle$. The upper limits of the error bars are estimated uncertainties whereas the lower limits denote $f_{obs}\langle\tau_{solv}\rangle$ in recognition of the unobserved dynamics in these systems. (If the uncertainty is larger than $(1 - f_{obs})\langle\tau_{solv}\rangle$, then the uncertainty is plotted instead.) The line shown here is the fit $\ln(\langle\tau_{solv}\rangle/s) = -26.40 + 1.20 \ln(\eta/cP)$ ($N = 66$, $R^2 = 0.91$, $\sigma_{fit} = 0.95$). The asterisk indicates data in $[N_{ip10,11}^+][Tf_2N^-]$.

In Figure 10 we compare values of $\langle\tau_{solv}\rangle$ measured in ionic liquids to values previously measured in conventional dipolar solvents at room temperature.[31,67] With the exception of the normal alcohols (n in Figure 10 denotes an alcohol with n C atoms) solvation times in most conventional solvents fall in the 1−10 ps range. The times observed in ionic liquids are much longer, typically in the 0.1−10 ns range. These longer solvation times can be partially understood in terms of the much larger viscosities of ionic liquids compared to those of conventional solvents. The solid line in Figure 10 shows a fit of all of the data to $\langle\tau_{solv}\rangle \propto \eta^p$ with $p = 1.2$. Clearly, viscosity differences rationalize the $>10^4$-fold variations in solvation times of C153, at least in a crude way. But the considerable scatter (10-fold differences for a given value of η) indicates that viscosity is not the only factor involved.

Solvation dynamics in conventional dipolar solvents has been studied for many years and is well understood.[30,31,83,84] There are two main reasons for the poor correlation between $\langle\tau_{solv}\rangle$ and η in such solvents. First, in many small-molecule dipolar solvents a substantial fraction of the total response comes from inertial contributions, and these contributions are not expected to be proportional to solvent viscosity. More importantly, dipolar solvation is a collective process whose time scale is determined both by the rate of individual solvent molecule motions, primarily rotation, and by the strength of the solvent−solvent coupling, or "polarity".[30,85] Because polarity is uncorrelated to solvent viscosity, except in homologous series such as the normal alcohols, solvent viscosity alone is unable to account for the variations in solvation times observed. But all of these factors are captured in the dielectric response, $\epsilon(\omega)$, of dipolar solvents, and solvation times of C153 in all of the dipolar solvents included in Figure 10 can be predicted with surprising accuracy from $\epsilon(\omega)$ and simple continuum models of solvation.[31,86]

Some authors have suggested that these same dielectric approaches might also be used to calculate solvation times in ionic liquids.[26,27,43] $\epsilon(\omega)$ data have been recently reported on a few ionic liquids,[26,27,49,87−89] and we have been able to make three detailed comparisons to date.[38,90] Like the solvation energy−ϵ_r comparisons in subsection 3A, the few available comparisons suggest that if any direct relationship exists between the solvation response and $\epsilon(\omega)$ in ionic liquids, then it is not the same as in dipolar liquids. In the absence of simple models and more dielectric data, we can at present only explore what correlations might exist between $\langle\tau_{solv}\rangle$ and other properties of these solvents.

The viscosity correlation shown in Figure 10 indicates the ionic liquid data fall into two main groupings. The solvation times of the majority (15) of the ionic liquids relate to viscosity in a way that is distinct from the 5 ionic liquids containing the $P_{14,666}^+$ cation. The single liquid $[N_{ip10,11}^+][Tf_2N^-]$ (marked with an asterisk in Figure 10) occupies an ambiguous position between these two groups. We note that this particular solvent exhibited considerably higher background emission than the other liquids studied, and we suspect that these points may be significantly affected by this background, which could not be entirely eliminated. Notwithstanding these errant points, we note that within either of the two main groups of solvents the correlation with viscosity is much better than it is in conventional solvents. For a given viscosity, however, the solvation times in the phosphonium liquids are about a factor of 5 slower than those in the main group of solvents. Another distinguishing feature of the dynamics in the phosphonium liquids is that essentially all of the solvation dynamics are observed ($f_{obs} \geq 93\%$). In most of the other liquids, even ones in which $\langle\tau_{solv}\rangle$ is greater than those of many of the phosphonium liquids, f_{obs} is much smaller. Thus, in contrast to most of the other liquids, those liquids containing the $P_{14,666}^+$ cation must lack substantial dynamics on the <25 ps time scale. We note that when the unresolved solvation components are considered the distinction between the two groups of liquids becomes larger. This fact can be appreciated from the lower error bounds shown in Figure 10, which are the products $f_{obs}\langle\tau_{solv}\rangle$. Whereas the points indicate measured values of $\langle\tau_{solv}\rangle$, which we take as the best estimates of the integral time of the diffusive component of the dynamics, the product $f_{obs}\langle\tau_{solv}\rangle$ is a lower limit to the integral time expected for the total response, including the inertial solvation component.

The most obvious characteristic that distinguishes the two groups of ionic liquids is cation size. As indicated by the ionic radii (R_+ and R_-) in Table 1, the $P_{14,666}^+$ ion is much larger than all of the other ions studied here. To investigate how ion size and other factors might control the observed solvation times, we have performed multilinear correlations of the logarithms of the solvation times to various measured and computed properties (viscosity, mass density, molar volume, molar refraction, and ion sizes) of these liquids. The best correlation that we have found is reproduced in Figure 11, which shows the relation $\langle\tau_{solv}\rangle \propto (\eta/T)^p R_+^q$ with $p = 1.04 \pm 0.04$ and $q = 4.1 \pm 0.2$. This correlation is reasonably accurate, with a standard error of ± 23% and only two points, one of the $[N_{ip10,11}^+][Tf_2N^-]$ points (15) and the lowest temperature datum in $[mIm_{31}^+][Tf_2N^-]$ (7), showing deviations of more than 50%. Because a number of related correlations provide comparable fits to the one shown here, we do not place much significance on the specific quantities (η/T) and R_+. For example, correlations with η rather than η/T and with R_{max}, the radius of the largest ion, rather than R_+ are of similar quality. What is clear from these analyses is that viscosity is the primary factor controlling the solvation time but that some measure of ion size (R_+ or R_{max}) is also needed to account for the split grouping shown in Figure 10. We find that ion size is better able to account for this split than bulk properties such as molar volume (equivalent to the $1/d$ used in subsection 3A) or density. It is also clear that

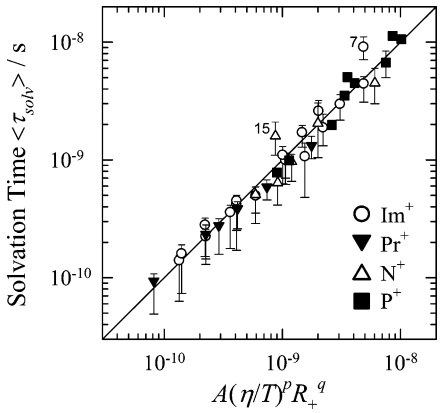

Figure 11. Correlation of the observed solvation times in ionic liquids $\langle\tau_{solv}\rangle$ with η/T and the cation radius R_+. Error bars are as in Figure 10. The correlation shown here represents the fit: $\ln(\langle\tau_{solv}\rangle/s) = \ln A + p \ln((\eta/cP)/(T/K)) + q \ln(R_+/Å)$ with $A = -25.15$, $p = 1.04$, $q = 4.97$ ($N = 39$, $R^2 = 0.97$, $\sigma_{fit} = 0.23$).

anion size R_- has virtually no effect on the quality of the correlations.

The interpretation of these correlations is not obvious. A relationship of the form $\langle\tau_{solv}\rangle \propto (\eta/T)R_+^3$ might be interpreted in terms of cation or largest ion reorientation or translational diffusion of the cation or the largest ion over some fraction of its size.[91] But an even stronger dependence on ion size than implied by such models, approximately R_+^4, is found here. On the basis of the important role of "polarity" via dipolar correlations[85,92] in determining solvation times in dipolar solvents, it is plausible that this additional dependence on ion size reflects some analogous influence of charge density in ionic liquids. But, if one neglects the ambiguous $[N_{ip10,11}^+][Tf_2N^-]$ data and simply treats the phosphonium liquids and all of the remaining ionic liquids as two distinct sets of data, then the data within each set are accounted for with equivalent accuracy without any explicit consideration of ion size. Thus, instead of attempting to rationalize the size dependence, it might be more profitable to assume that some qualitative distinction exists between the liquids incorporating the large $P_{14,666}^+$ cation and the remaining ionic liquids. As already noted, the phosphonium ionic liquids also show some distinctive behavior both with respect to the energies $\Delta_{sol}G$ (Figure 3) and with respect to the nonexponentiality of C153 reorientations (β_{rot}; Table 4). We conjecture that the long 14-carbon chain of $P_{14,666}^+$ might lead to extensive polar/nonpolar domain formation of the sort uncovered in computer simulations.[80,81] Support for such structures comes from previous studies that show that phosphonium ionic liquids with long alkyl chains tend to form layered crystals and liquid crystalline phases in which ionic and nonpolar domains segregate into planar arrays.[93−95] The slower than expected solvation of C153 in phosphonium ionic liquids might be associated with slow domain relaxation kinetics or possibly solute diffusion among different domains. Clearly more study of the phosphonium liquids is required to decide the correctness of this idea.

3. Summary and Conclusions

We have used steady-state and time-resolved emission spectroscopy to measure static and dynamic aspects of the solvation of C153 in 21 different ionic liquids and compared these results to what is observed in conventional dipolar solvents. In keeping with the findings of many prior studies of solvatochromism in ionic liquids,[3,8] the electronic shifts of C153 report "polarities" of the ionic liquids studied here to be comparable to those in highly polar conventional solvents. This polarity, as reported by the energetic quantities $\Delta_{sol}G$ and λ_{sol}, is not simply related to solvent permittivity ϵ_r as it is in conventional solvents. These quantities instead appear to be correlated with some measure of ion density or mean ion separation. It seems likely that simple models akin to dielectric continuum models for dipolar solvents can be developed to understand dipole solvation in ionic liquids.

Beyond the considerable reduction in rotation rates caused by the larger viscosities of ionic liquids, rotation of C153 appears much the same in ionic liquids and conventional solvents. The rotation times of C153 in ionic liquids follow the expected η/T dependence and show comparable frictional coupling in ionic liquids and conventional dipolar solvents. Rotational correlation functions in ionic liquids are usually not single-exponential functions of time as they often are in low-viscosity conventional solvents. However, in most cases we suspect that this difference can be attributed to non-Markovian friction effects[76] that are more evident in ionic liquids because of their higher viscosities rather than to any special features of the ionic liquid environment. An exception might be in the phosphonium ionic liquids, where the nonexponentiality of the rotational correlation functions is much greater than that observed in the remaining liquids. It is interesting to note that even in these latter liquids the rotational correlation times observed are close to what is expected based on stick hydrodynamic calculations. This observation is consistent with the rotation times of a number of different fluorescence probes in $[Im_{41}^+][PF_6^-]$[21] and other liquids.[17,22−29] It stands in marked contrast to emerging dielectric[88,96] and NMR results[97] of rotation times of the ionic liquid constituents themselves, which have been interpreted as indicating 20−50 times faster rotation of imidazolium cations compared to hydrodynamic expectations.

Solvation dynamics of C153 in ionic liquids occur over a broad range of time scales, and for this reason, only a portion of the total response can typically be captured using TCSPC.[37,38] Nevertheless, the use of TCSPC is expected to provide reliable values for the integral solvation times associated with the noninertial component of solvation.[38] The survey of such times presented here shows that a single parameter, the solvent viscosity, suffices to correlate solvation times in the majority of the ionic liquids studied with an average accuracy of about 25%. This connection to viscosity has been noted in a number previous studies,[18,19,36,41] but given the variety of cations and anions included in the present data set (15 ionic liquids) the quality of this single-parameter correlation is remarkable. We note that a number of other groups have measured solvation times of C153 in solvents other than those studied here.[29,33,34,40,41,46] In light of the variability of samples and analysis methods among different laboratories[21,40] we have not attempted to include any of these data in the present compilations. However, it is worth mentioning that the recent data of Castner and co-workers[29] in two ammonium and two pyrrolidinium ionic liquids at six temperatures follow the same correlation with viscosity as do the majority of ionic liquids studied here.[98] The only clear deviations that we find from this general correlation with viscosity are in ionic liquids containing the large $P_{14,666}^+$ cation. Within this set of solvents there is also a good correlation between solvation times and viscosity, but here the solvation times are about 5-fold slower for a given viscosity than in the remaining liquids. This dichotomy can be viewed as a result of an either explicit cation size dependence of the solvation dynamics or as the result of some qualitative difference in these phosphonium ionic liquids. We favor the

latter viewpoint and propose that some domain-like structure, induced by the long 14-carbon chain of the cation, leads to distinctive behavior in both the solvation and rotation of C153 in these liquids.

Acknowledgment. The authors thank Ed Castner, Hermann Weingärtner, and Jacob Petrich for preprints of their work as well as for many helpful discussions. This work was supported by a grant from the Chemical Sciences, Geosciences, and Biosciences Division, Office of Basic Energy Science, U. S. Department of Energy.

References and Notes

(1) Freemantle, M. *Chem. Eng. News* **2007**, *85* (1), 23−26.
(2) Endres, F.; El Abedin, S. Z. *Phys. Chem. Chem. Phys.* **2006**, *8*, 2101−2116.
(3) Chiappe, C.; Pieraccini, D. *J. Phys. Org. Chem.* **2005**, *18*, 275−297.
(4) Handy, S. T. *Curr. Org. Chem.* **2005**, 959−988.
(5) Wasserscheid, P.; Welton, T., Eds. *Ionic Liquids in Synthesis*; Wiley-VCH: Weinheim, Germany, 2003.
(6) Abraham, M.; Acree, W. E. *Green Chem.* **2006**, *8*, 906−915.
(7) Crosthwaite, J. M.; Muldoon, M. J.; Aki, S. N. V. K.; Maginn, E. J.; Brennecke, J. F. *J. Phys. Chem. B* **2006**, *110*, 9354−9361.
(8) Poole, C. F. *J. Chromatogr., A* **2004**, *1037*, 49−82.
(9) Eike, D. M.; Brennecke, J. F.; Maginn, E. J. *Ind. Eng. Chem. Res.* **2004**, *43*, 1039−1048.
(10) Diedenhofen, M.; Eckert, F.; Klamt, A. *J. Chem. Eng. Data* **2003**, *48*, 475−479.
(11) Anderson, J. L.; Ding, J.; Welton, T.; Armstrong, D. W. *J. Am. Chem. Soc.* **2002**, *124*, 14247−14254.
(12) Mellein, B. R.; Aki, S. N. V. K.; Ladewski, R. L.; Brennecke, J. F. *J. Phys. Chem. B* **2007**, *111*, 131−138.
(13) Reichardt, C. *Green Chem.* **2005**, *7*, 339−351.
(14) Werner, J. H.; Baker, S. N.; Baker, G. A. *Analyst* **2003**, *126*, 786−789.
(15) Morgan, D.; Ferguson, L.; Scovazzo, P. *Ind. Eng. Chem. Res.* **2005**, *44*, 4815−4823.
(16) Evans, R. G.; Klymenko, O. V.; Price, P. D.; Davies, S. G.; Hardacre, C.; Compton, R. G. *ChemPhysChem* **2005**, *6*, 526−533.
(17) Baker, S. N.; Baker, G. A.; Kane, M. A.; Bright, F. V. *J. Phys. Chem. B* **2001**, *105*, 9663−9668.
(18) Ingram, J. A.; Moog, R. S.; Ito, N.; Biswas, R.; Maroncelli, M. *J. Phys. Chem. B* **2003**, *107*, 5926−5932.
(19) Arzhantsev, S.; Ito, N.; Heitz, M.; Maroncelli, M. *Chem. Phys. Lett.* **2003**, *381*, 278−286.
(20) Ito, N.; Arzhantsev, S.; Heitz, M.; Maroncelli, M. *J. Phys. Chem. B* **2004**, *108*, 5771−5777.
(21) Ito, N.; Arzhantsev, S.; Maroncelli, M. *Chem. Phys. Lett.* **2004**, *396*, 83−91.
(22) Chakrabarty, D.; Hazra, P.; Chakraborty, A.; Seth, D.; Sarkar, N. *Chem. Phys. Lett.* **2003**, *381*, 697−704.
(23) Chakrabarty, D.; Chakraborty, A.; Seth, D.; Hazra, P.; Sarkar, N. *Chem. Phys. Lett.* **2004**, *397*, 460−474.
(24) Chakraborty, A.; Seth, D.; Chakrabarty, D.; Setua, P.; Sarkar, N. *J. Phys. Chem. A* **2005**, *109*, 11110−11116.
(25) Mali, K. S.; Dutt, G. B.; Mukherjee, T. *J. Chem. Phys.* **2005**, *123*, 174504.
(26) Ito, N.; Huang, W.; Richert, R. *J. Phys. Chem. B* **2006**, *110*, 4371−4377.
(27) Ito, N.; Richert, R. *J. Phys. Chem. B* **2006**, *111*, 5016−5022.
(28) Paul, A.; Samanta, A. *J. Phys. Chem. B* **2007**, *111*, 4724−4731.
(29) Funston, A. M.; Fadeeva, T. A.; Wishart, J. F.; Castner, E. W., Jr. *J. Phys. Chem. B* **2007**, *111*, 4963−4977.
(30) Stratt, R. M.; Maroncelli, M. *J. Phys. Chem.* **1996**, *100*, 12981−12996.
(31) Horng, M. L.; Gardecki, J. A.; Papazyan, A.; Maroncelli, M. *J. Phys. Chem.* **1995**, *99*, 17311−17337.
(32) Karmakar, R.; Samanta, A. *J. Phys. Chem. A* **2002**, *106*, 4447−4452.
(33) Karmakar, R.; Samanta, A. *J. Phys. Chem. A* **2002**, *106*, 6670−6675.
(34) Karmakar, R.; Samanta, A. *J. Phys. Chem. A* **2003**, *107*, 7340−7346.
(35) Saha, S.; Mandal, P. K.; Samanta, A. *Phys. Chem. Chem. Phys.* **2004**, *6*, 3106−3110.
(36) Mandal, P. K.; Samanta, A. *J. Phys. Chem. B* **2005**, *109*, 15172−15177.
(37) Arzhantsev, S.; Jin, H.; Ito, N.; Maroncelli, M. *Chem. Phys. Lett.* **2006**, *417*, 524−529.
(38) Arzhantsev, S.; Jin, H.; Baker, G. A.; Maroncelli, M. *J. Phys. Chem. B* **2007**, *111*, 4978−4989.
(39) Chakrabarty, D.; Chakraborty, A.; Seth, D.; Sarkar, N. *J. Phys. Chem. A* **2005**, *109*, 1764−1769.
(40) Chowdhury, P. K.; Halder, M.; Sanders, L.; Calhoun, T.; Anderson, J. L.; Armstrong, D. W.; Song, X.; Petrich, J. W. *J. Phys. Chem. B* **2004**, *108*, 10245−10255.
(41) Headley, L. S.; Mukherjee, P.; Anderson, J. L.; Ding, R.; Halder, M.; Armstrong, D. W.; Song, X.; Petrich, J. W. *J. Phys. Chem. A* **2006**, *110*, 9549−9554.
(42) Mukherjee, P.; Crank, J. A.; Halder, M.; Armstrong, D. W.; Petrich, J. W. *J. Phys. Chem. A* **2006**, *110*, 10725−10730.
(43) Halder, M.; Headley, L. S.; Mukherjee, P.; Song, X.; Petrich, J. W. *J. Phys. Chem. A* **2006**, *110*, 8623−8626.
(44) Baker, S. N.; Baker, G. A.; Munson, C. A.; C., F.; Bukowski, E. J.; Cartwright, A. N.; Bright, F. V. *Ind. Eng. Chem. Res.* **2003**, *42*, 6457−6463.
(45) Lang, B.; Angulo, G.; Vauthey, E. *J. Phys. Chem. A* **2006**, *110*, 7028−7034.
(46) Samanta, A. *J. Phys. Chem. B* **2006**, *110*, 13704−13716.
(47) Mandal, P. K.; Saha, S.; Karmakar, R.; Samanta, A. *Curr. Sci.* **2006**, *90*, 301−310.
(48) Weingärtner, H. *Z. Phys. Chem.* **2006**, *220*, 1395−1405.
(49) Schrödle, S.; Annat, G.; MacFarlane, D. R.; Forsyth, M.; Buchner, R.; Hefter, G. *Chem. Commun.* **2006**, 1748−1750.
(50) Wu, J.; Stark, J. P. W. *Meas. Sci. Technol.* **2006**, *17*, 781−788.
(51) Behar, D.; Neta, P.; Schultheisz, C. *J. Phys. Chem. A* **2002**, *106*, 3139−3147.
(52) Bradaric, C. J.; Downard, A.; Kennedy, C.; Robertson, A.; Zhou, Y. *Green Chem.* **2003**, *5*, 143−152.
(53) Baker, S. N.; McCleskey, T. M.; Pandey, S.; Baker, G. A. *Chem. Commun.* **2004**, 940−941.
(54) Jin, H.; O'Hare, B.; Dong, J.; Arzhantsev, S.; Baker, G. A.; Wishart, J. F.; Benesi, A.; Maroncelli, M. *J. Phys. Chem. B*, to be submitted for publication.
(55) We had available one of the phosphonium ionic liquids, $[P_{14,666}^+][Tf_2N^-]$, used for making the measurements reported in ref 20. Because our ability to dry and measure water content has improved significantly since that earlier work, we dried the $[P_{14,666}^+][Tf_2N^-]$ (to <30 ppm water) and remeasured the solvation dynamics at 298 K. The results obtained with this drier sample were well within the experimental uncertainties of the earlier results.
(56) Gardecki, J. A.; Maroncelli, M. *Appl. Spectrosc.* **1998**, *52*, 1179−1189.
(57) Heitz, M. P.; Maroncelli, M. *J. Phys. Chem. A* **1997**, *101*, 5852−5868.
(58) Maroncelli, M.; Fleming, G. R. *J. Chem. Phys.* **1987**, *86*, 6221−6239.
(59) Cross, A. J.; Fleming, G. R. *Biophys. J.* **1984**, *46*, 45−56.
(60) Baker, S. N.; Baker, G. A.; Bright, F. V. *Green Chem.* **2002**, *4*, 165−169.
(61) Huddleston, J. G.; Broker, G.; Willauer, H.; Rogers, R. D. In *Ionic Liquids: Industrial Applications for Green Chemistry*; Rogers, R. D., Seddon, K. R., Eds.; ACS Symposium Series 818; American Chemical Society: Washington, DC, 2002; pp 270−288.
(62) Crowhurst, L.; Mawdsley, P. R.; Perez-Arlandis, J.; Salter, P. A.; Welton, T. *Phys. Chem. Chem. Phys.* **2003**, *5*, 2790−2794.
(63) Carmichael, A. J.; Seddon, K. R. *J. Phys. Org. Chem.* **2000**, *13*, 591−595.
(64) Ogihara, W.; Aoyama, T.; Ohno, H. *Chem. Lett.* **2004**, *33*, 1414−1415.
(65) Muldoon, M. J.; Gordon, C. M.; Dunkin, I. R. *J. Chem. Soc., Perkin Trans. 2* **2001**, 433−435.
(66) Fletcher, K. A.; Storey, I. A.; Hendricks, A. E.; Pandey, S.; Pandey, S. *Green Chem.* **2001**, *3*, 210−215.
(67) Reynolds, L.; Gardecki, J. A.; Frankland, S. J. V.; Horng, M. L.; Maroncelli, M. *J. Phys. Chem.* **1996**, *100*, 10337−10354.
(68) Fletcher, K. A.; Pandey, S.; Storey, I. K.; Hendricks, A. E.; Pandey, S. *Anal. Chim. Acta* **2002**, *453*, 89−96.
(69) Fee, R. S.; Maroncelli, M. *Chem. Phys.* **1994**, *183*, 235−247.
(70) Krossing, I.; Slattery, J. M.; Daguenet, C.; Dyson, P. J.; Oleinkova, A.; Weingärtner, H. *J. Am. Chem. Soc.* **2006**, *128*, 13427−13434.
(71) It should be noted that Wu and Stark[50] have reported a value of 69.9 ±.7 for $[Im_{41}^+][BF_4^-]$ using a new method that they propose for measuring permittivities of conducting materials. This value differs greatly from the value of 11.7 of Weingärtner and co-workers,[48] which we take to be more reliable.
(72) Khajehpour, M.; Kauffman, J. *J. Phys. Chem. A* **2000**, *104*, 9512−9517.
(73) Glasser, L.; Jenkins, D. H. B. *Chem. Soc. Rev.* **2005**, *34*, 866−874.

(74) In an attempt to observe kinetic heterogeneity we measured anisotropies of C153 in $[N_{ip311}^+][Tf_2N^-]$ at 298 K using excitation wavelengths of 410, 420, 430, 440, 450, and 460 nm (emission observed near steady-state emission maximum). We found the integral rotation times to be 6.0 ± 0.2 ns with no systematic variation in the times or the nonexponentialities (β_{rot}) of the decays.

(75) Allowing this parameter to vary in the fitting procedure typically yielded values between 0.36 and 0.38. However, in some cases allowing this parameter to vary led to significantly different values. For consistency we therefore fixed the value to 0.375, which was determined from the value in a glassy medium determined in ref 76.

(76) Horng, M.-L.; Gardecki, J.; Maroncelli, M. *J. Phys. Chem. A* **1997**, *101*, 1030−1047.

(77) Ito, N.; Kajimoto, O.; Hara, K. *J. Phys. Chem. A* **2002**, *106*, 6024−6029.

(78) Cicerone, M. T.; Blackburn, F. R.; Ediger, M. D. *J. Chem. Phys.* **1995**, *104*, 471−479.

(79) Yang, M.; Richert, R. *Chem. Phys.* **2002**, *284*, 103−114.

(80) Lopes, J. N. C.; Padua, A. A. H. *J. Phys. Chem. B* **2006**, *110*, 3330−3335.

(81) Wang, Y.; Voth, G. A. *J. Phys. Chem. B* **2006**, *110*, 18601−18608.

(82) Three direct comparisons can be made. In $[Im_{41}^+][PF_6^-]$ at 298 K, Sarkar and co-workers reported C153 rotation times of 4.7[24] and 3.57 ns[22] ($r_0 \approx 0.25$), much shorter times than the 12 ± 2 ns measured here. The reason for this large difference is unclear. Funston et al.[29] measured temperature-dependent rotation times of C153 in $[N_{4441}^+][Tf_2N^-]$ and $[Pr_{41}^+][Tf_2N^-]$. Interpolating their data to 298 K provides values of 28 ns in both cases. Our value of 51 ± 25 ns in $[N_{4441}^+][Tf_2N^-]$ at 298 K is poorly defined but in general agreement with their more accurate determination. In $[Pr_{41}^+][Tf_2N^-]$ we measure 3.4 ± 0.5 ns, which is quite far from their correlation time of 28 ns. However, their large correlation time reflects the presence of a ∼200 ns component whose reality is presently uncertain and that would be impossible to detect in our experiments. If this component is neglected, then their time reduces to 3.8 ns, in agreement with our value.

(83) Raineri, F. O.; Friedman, H. L. *Adv. Chem. Phys.* **1999**, *107*, 81−189.

(84) Kapko, V.; Egorov, S. A. *J. Chem. Phys.* **2004**, *121*, 11145−11155.

(85) Maroncelli, M.; Kumar, V. P.; Papazyan, A. *J. Phys. Chem.* **1993**, *97*, 13−17.

(86) Maroncelli, M. *J. Chem. Phys.* **1997**, *106*, 1545−1555.

(87) Weingärtner, H.; Knocks, A.; Schrader, W.; Kaatze, U. *J. Phys. Chem. A* **2001**, *105*, 8646−8650.

(88) Daguenet, C.; Dyson, P. J.; Krossing, I.; Oleinikova, A.; Slattery, J.; Wakai, C.; Weingärtner, H. *J. Phys. Chem. B* **2006**, *110*, 12682−12688.

(89) Weingärtner, H.; Sasisanker, P.; Daguenet, C.; Dyson, P. J.; Krossing, I.; Slattery, J. M.; Schubert, T. *J. Phys. Chem. B* **2007**, *111*, 4775−4780.

(90) Halder et al.[43] have made a similar comparison in a fourth ionic liquid with apparently more satisfactory agreement between experiment and dielectric continuum calculations. However, their calculations ignore the missing fast components of $\epsilon(\omega)$. Although the dielectric measurements that they employ extend to 90 GHz, even here when unobserved components in $\epsilon(\omega)$ are accounted for in the approximate manner described in ref 38, the level of agreement between the calculated and observed solvation response is significantly degraded.

(91) Diffusion of a cation over a time t leads to an average squared displacement of $\langle r_+^2 \rangle = 6D_+t$ with $D_+ \cong k_BT/6\pi\eta R_+$. The time required to diffuse a distance proportional to the size of a cation is therefore proportional to $(\eta/T)R_+^3$.

(92) Ladanyi, B. M.; Maroncelli, M. *J. Chem. Phys.* **1998**, *109*, 3204−3221.

(93) Abdallah, D. J.; Robertson, A.; Hsu, H. F.; Weiss, R. G. *J. Am. Chem. Soc.* **2000**, *122*, 3053−3062.

(94) Chen, H.; Kwait, D. C.; Gonen, Z. S.; Weslowski, B. T.; Abdallah, D. J.; Weiss, R. G. *Chem. Mater.* **2002**, *14*, 4063−4072.

(95) On the basis of observing anomalously small activation energies for rotation of an electron spin resonance probe Evans et al.[99] suggested that such a bilayer structure exists in $[P_{14,666}^+][Tf_2N^-]$ and a related $P_{14,666}^+$ ionic liquid. The simple volumetric behavior observed of $[P_{14,666}^+][Tf_2N^-]$ and other $P_{14,666}^+$ liquids[100] would seem to argue against anything so highly organized. It could be that the unusual behavior observed by Evans et al.[99] might result from the reorientation being highly nonexponential in these liquids, which could invalidate the line shape analysis used.

(96) Schröder, C.; Wakai, C.; Weingärtner, H.; Steinhauser, O. *J. Chem. Phys.* **2007**, *126*, 84511.

(97) Wulf, A.; Ludwig, R.; Sasisanker, P.; Weingärtner, H. *Chem. Phys. Lett.* **2007**, *439*, 323−326.

(98) The collected data of Funston et al.[29] as a function of viscosity show roughly the same amount of scatter as the majority grouping of solvents in Figure 10. The only clear deviation occurs for the two highest viscosity points (η > 3000 cP) where the times that they report (∼10 ns) are roughly a factor of 3 faster than expected.

(99) Evans, R. G.; Wain, A. J.; Hardacre, C.; Compton, R. G. *ChemPhysChem* **2005**, *6*, 1035−1039.

(100) Esperanca, J. M. S. S.; Guedes, H. J. R.; Blesic, M.; Rebelo, L. P. N. *J. Chem. Eng. Data* **2006**, *51*, 237−242.